Design and construction of an apparatus to visualize incompressible fluid flow in several regimes

F. Iturbide Jiménez, A.J. Mendoza Jasso, A. Antonio García, and A. Santiago Alvarado
Universidad Tecnológica de la Mixteca,
Carretera a Acatlima Km. 2.5 Huajuapan de León, Oaxaca, C.P. 69000.

In this work, the design and construction of a didactic experimental equipment to visualize the fluid flow behavior in the laminar, transition and turbulent regimes is presented; as well as the ability to measure and display the respective Reynolds number (Re) of each flow; current educational equipments have limited or null capacity in this regard. The equipment was designed taking into account the basic laws of fluids such as mass, momentum and energy conservation. The analytical calculations were numerically validated using the finite element method (FEM), for which the Ansys software was used in its Ansys® Parametric Design Language (APDL) and Workbench platforms. Solidworks tools for conceptual design and Stratasys Catalist for three dimension (3D) printing were used. Additionally, hardware was implemented for the step of measuring the flow velocity, temperature and Re calculation. The apparatus is a valuable resource in fluid flow visualization since it permits to read several fluid parameters immediately from a display.

Keywords: Fluid regimes; fluid visualization; simulation.

PACS: 01; 07; 47

1. Introducction

Flow of liquids or gases is commonly present in heating, chilling and hydraulic distribution network systems, where a typical array includes pipes of several diameters, valves, different types of fittings and pumps, where these devices are used to pressurize flow, control flux and change flow's direction. Even though the theory of fluid flow is reasonably understood, theoretical solutions are found only for some simple cases, such as laminar flow completely developed in a circular pipe. Therefore, theory should be backed up with experimental results and empiric relations for many of fluid flow problems, instead of having exclusively analytical solutions. On the other hand, it is important to observe fluid behaviour at different velocities to clearly comprehend fluid phenomena, which is characterized by the dimensionless Reynolds number.

Development of the system proposed in this work was carried out following the Product design and development (PDD) methodology depicted in Fig. 1.
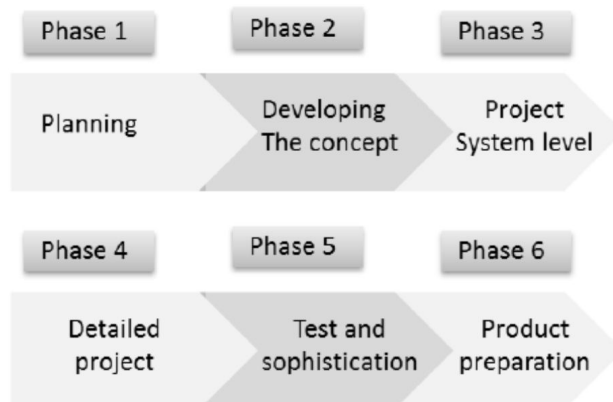

FIGURE 1. Main phases of PDD process.

2. Equipment design concept development and detail

Design process consists on converting needs and requirements into useful products. Problem is looked into and project's scope is defined. In this stage, the factors discussed in the following sections were taken into account to come up with the proposed equipment shown in Fig. 2.

2.1. Water containers

The prototype includes two water containers or tanks, the first container is connected to a pump which provides it with water. The second container is divided into three sections. The first section is filled up with water coming from the first container so that turbulence caused by water dropping does not affect the other sections.

A thermometer is connected in this section to collect data for density and viscosity calculations. When water fills the first section completely and reaches the high of a wall that
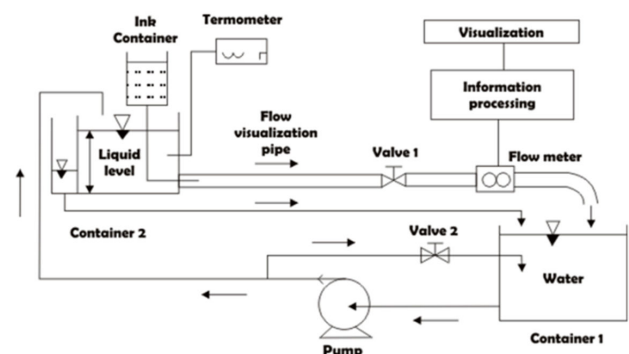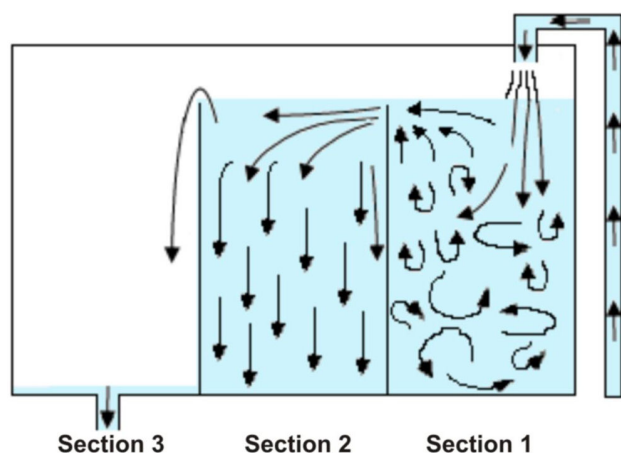

FIGURE 2. Conceptual scheme of the proposed system.

FIGURE 3. Arrangement of sections in container 2.

separates sections, it starts to drain to the next section without causing turbulence since it flows smoothly over the division. The second section provides the necessary fluid for the experiment; when fluid has constant height, experiment is started by opening valve 1 to permit the liquid to flow across a visualization pipe and through a flow meter to know flow velocity. In this section flow behaviour is observed by injecting ink in order to color stream lines. The fluid in the second section eventually will fill and drain to the third section and will then return to the first container to start the cycle all over again, Fig. 3.

2.2. Diameter selection of visualization pipe

Piping dimensions were calculated based in the following equipment and their characteristics: water pump, flow meter and material of visualization pipes, either glass or acrylic.

2.3. Water pump selection

According to the usage of this device, the pump selected is of submersible type, lightweight, easy installation, silent and with a capacity of 2.92×10^{-4} m^3 s^{-1} (Fig. 4a).

2.4. Flow meter

Hall flow meter type was selected (Fig. 4b), which consists in a turbine that spins when fluid crosses it and produces a se-
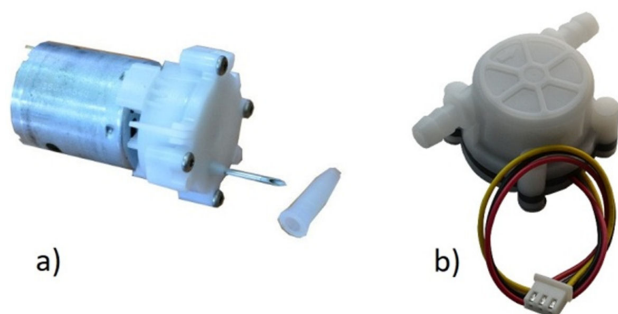
ries of pulses that are proportional to the flux passing through a sensor. Commercially, flow meter with nominal diameter 12.7 mm is able to measure in the range 8.33×10^{-6} to 5×10^{-4} m^3 s^{-1}, and the 25.4 mm flow meter can deal with 3.33×10^{-5} up to 1.67×10^{-3} m^3 s^{-1}.

2.5. Pipe selection

Commercially available transparent pipes, made either of glass or acrylic and able to connect adequately to flow meters have 12.7, 19.05 and 25.4 mm in diameter. Consequently, an analysis was carried out to determine the interval of Re numbers that might be visualized and measured for the different combinations of diameters and flux sensors, based on the minimum fluxes that sensors were able to detect and the maximum volume displaced by the pump, taking into account material's roughness [14].

Combination of 19.05 mm pipe and 12.7 mm flow meter gave the largest interval of Reynolds numbers to be measured in this equipment (Fig. 5). Such range includes Re numbers from 800 up to 28000.

Another important aspect in the design of this system is the length of the visualization pipe. Such length is determined by taking into account the inlet length Le, which is the region where the flux has not yet developed completely.

Velocity profile in the region where flow is totally developed has a parabolic shape in laminar flow, and it is flatter in turbulent regime due to vortex movement and vigorous flow mix in radial direction (Fig. 6).
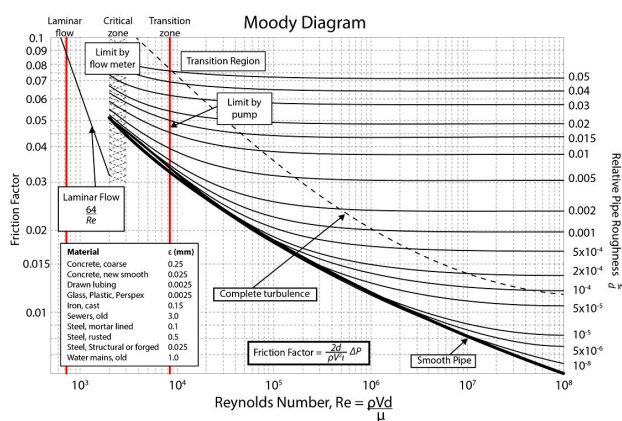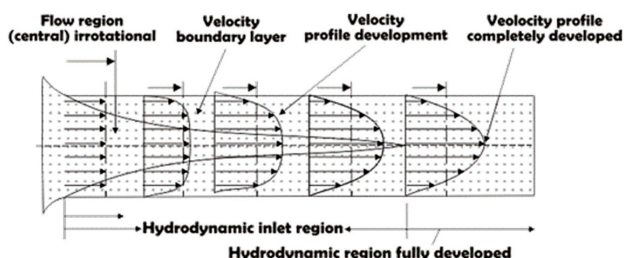

FIGURE 5. Range of Re numbers for flow meter of 1/2" and pipe of 3/4" [21].

FIGURE 4. Flow meter YF-S201: a) pump, b) flow meter [16].

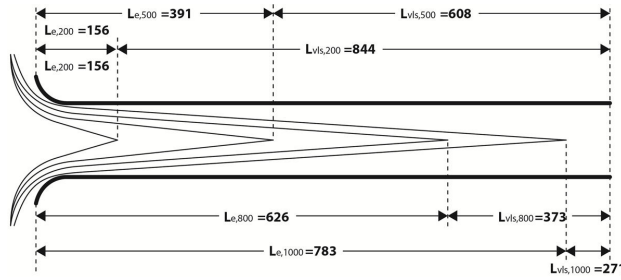FIGURE 6. Input lengths and development of velocity profile.

FIGURE 7. Laminar flow inlet lengths.

In laminar regime, hydrodynamic inlet length Le_{lam} is approximated with the following expression [1-4]:
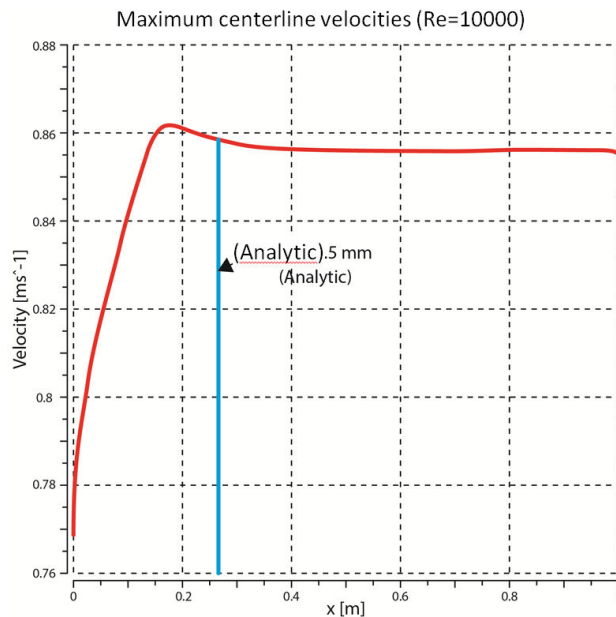
$$\frac{Le_{lam}}{d} \approx 0.006 Re \qquad (1)$$

where Re is the Reynolds number and d is the pipe diameter. In turbulent regime, the intense mixture during random fluctuations usually hides molecular diffusion effects. Inlet length for turbulent flow Le_{turb} is approximated with [1-4]:

$$\frac{Le_{turb}}{d} \approx 4.4 Re^{1/6} \qquad (2)$$

Figure 7 shows theoretical inlet lengths (in mm) needed to develop completely the velocity profiles that correspond to laminar Reynolds numbers ($L_{Reynolds} = L_{ent}$) for different design conditions; visualization lengths are also shown for each inlet lenght. For turbulent flows, it was observed that profiles are closer to each other than in the case of laminar flow.

A 1000 mm pipe was selected from these results. These measurements were corroborated with a finite element analysis [5-9] ran in ANSYS® for different Reynolds numbers: 800, 1000, 4000 and 10000.

FIGURE 8. Simulation results of velocity change along pipe's centerline for $Re = 10000$, Ansys® Fluent.

Velocities for each Reynolds numbers (inlet condition, left hand arrows), atmospheric pressure (outlet condition, right hand arrows) and walls (pipe) dimensions were taken as boundary parameters for the simulation.

Results from ANSYS® Fluent for Reynolds number of 10000 are shown in Fig. 8 as an example. Velocity change throughout centerline of the pipe can be seen in red; when fluid reaches the inlet length, velocity becomes constant. Both numerical and analytical results are presented in the figure. After velocity profile surpassed the inlet length, it remains constant for the rest of the pipe.

2.6. Calculation of heights

Energy conservation equation is used to know the heights between any points 1 and 2 [1-3], necessary to know velocities that the system will be able to reach (Fig. 10).

$$\frac{P_1}{\gamma} + \frac{V_1^2}{2g} + H_1 + H_2 = \frac{P_2}{\gamma} + \frac{V_2^2}{2g}$$
$$+ h_f + \sum h_m \qquad (3)$$

Where P is pressure, V is speed, H is elevation from a reference, g is acceleration due to gravity, h is the hydraulic head and γ is the specific weight. Considering changes in diameters, lengths and energy losses in each section between 1 and 2, energy equation reads:

$$H1 + H2 = \frac{V_1^2}{2g} \left\{ \left(f_1 \frac{L_1}{d_1} + K_{cg} \right) + \left(\frac{d_1}{d_2} \right)^4 (K_{eb} + K_{cb}) \right.$$
$$+ \left(\frac{d_1}{d_3} \right)^4 \left(f_3 \frac{L_3}{d_3} \right) + \left(\frac{d_1}{d_4} \right)^4 (K_v)$$
$$\left. + \left(\frac{d_1}{d_5} \right)^4 \left(f_5 \frac{L_5}{d_5} + K_c + 1 \right) \right\} \qquad (4)$$

where K_i are energy losses due to system's features: K_{cg} denotes gradual contractions, K_f indicates friction, K_v relates
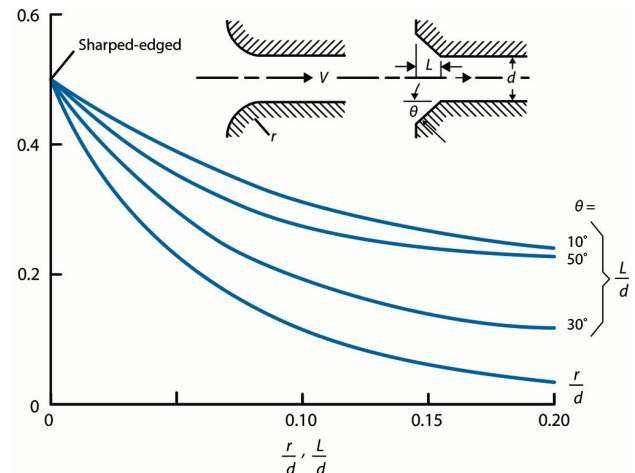

FIGURE 9. Losses diagram for gradual contraction factor K_{cg}.

TABLE I. Height calculation for different Reynolds numbers.

Reynolds	V_1 (ms^{-1})	f_1	f_2	$f_{3,5}$	H_1+H_2 (m)
15000	1.15	0.02786	0.02672	0.03027	0.4433
17000	1.30	0.02699	0.02591	0.02928	0.5625
20000	1.54	0.02593	0.02492	0.02806	0.7668
23000	1.77	0.02506	0.02412	0.02708	1.0014
25000	1.92	0.02457	0.02366	0.02655	1.1746
28000	2.15	0.02393	0.02306	0.02578	1.4595

to valve, K_{eb} and K_{cb} are losses in flow sensor and K_c means 90° bends.

In the case of K_{cg}, a relation $r = d > 1$ was proposed for gradual connections in the equipment, where r is the radio of the fillet and d the diameter of the pipe, Fig. 9. Friction losses are calculated for flow in turbulent state since it is not possible to know valve's opening size [10-13] and the maximum height of equipment corresponds to the largest Reynolds number, *i.e.*, in turbulent regime.

A friction factor value $\epsilon = 0.0015$ mm is considered for extruded plastic to compute friction loss; the length of the acrylic pipe is 1000 mm. Polyvinyl chloride PVC pipes of 12.7 mm in diameter and 150 mm in length are used to join flow meter with the valve, and the valve with the elbow.

As the Reynolds number grows, height H_1+H_2 also increases because more potential energy is needed to accelerate the fluid. Table I shows this behavior.

From an optimization point of view, a height of 1.0 m is chosen for this testing equipment, expecting to obtain a maximum Reynolds number of 23000 and a visualization velocity in the pipe of 1.77 m s^{-1}. Once system's configuration is set, simulations are carried out in Ansys® Workbench (Fig. 10). Simulation results were used to build a system's prototype. Boundary conditions are: atmospheric pressure at inlet and outlet points, pipe's wall, and gravitational acceleration equals -9.81 m s^{-2} in vertical direction. Simulation's results give the velocities at different sections in the system.

Figure 10 shows flow simulation through the system. Results highlight that velocity in the visualization pipe is close
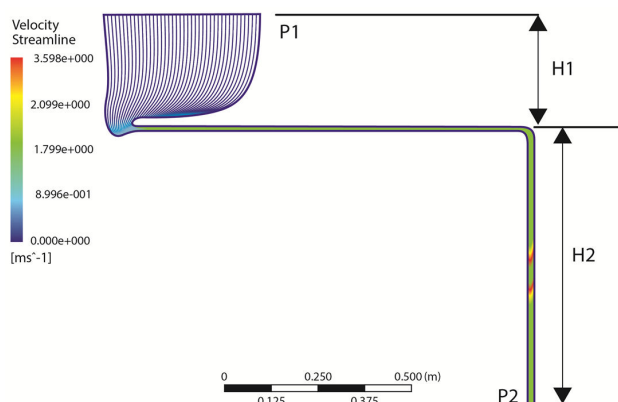
to 1.79 m s^{-1} which is slightly above the analytical result of 1.77 m s^{-1}.

Velocities V_2 through V_5 in each section of piping are calculated using the equation of continuity, for example, for Sec. 2, $V_2 = V_1(d_1^2/d_2^2)$, and on substituting $V_1 = 1.77$ m s^{-1}:

$$V_{2,4,5} = 0.93 \text{ m s}^{-1}, \qquad V_3 = 2.49 \text{ m s}^{-1}$$

Comparison of these values with simulations in Fig. 10, demonstrates that both values match for every section.

3. Equipment construction and testing

Scheme in Fig. 11 shows the various equipment's subsystems. Construction of equipment required the use of additive manufacturing (3D printing), Computer Aided Manufacturing (CAM) and conventional cutting and assembly processes.

Figure 12 displays final design after construction of parts and assembly [15-19].

Figure 13 exhibits how the equipment is used to visualize fluid at three types of flow regimes by injecting ink to the fluid. The equipment has maximum measures of 0.60 m wide by 1.20 m long and 1.20 m high.
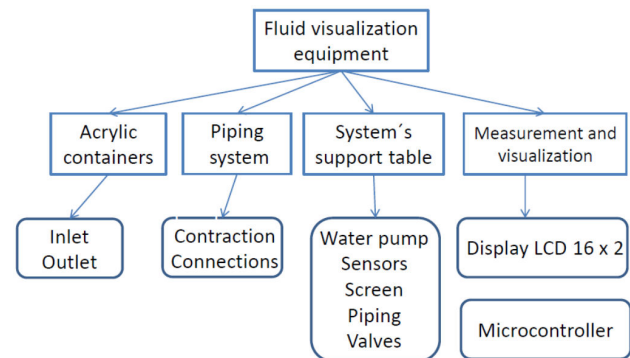

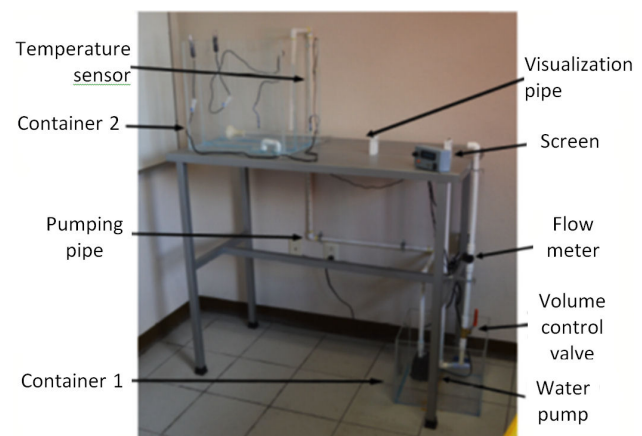FIGURE 11. Diagram of equipment's subsystems.

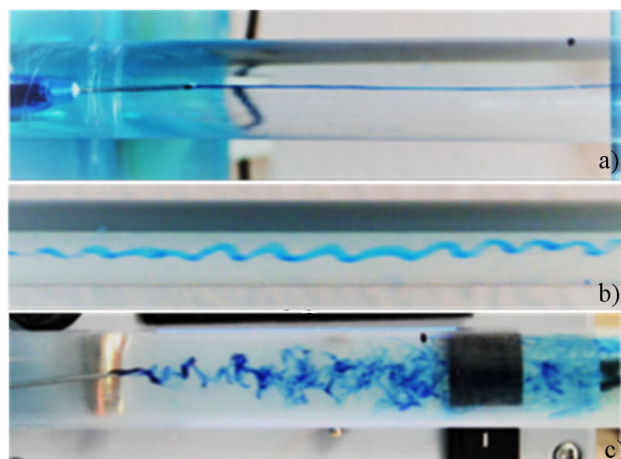FIGURE 10. Velocity distribution in the system.

FIGURE 12. Equipment assembled.

FIGURE 13. Flow visualization: a) laminar, b) transition and c) turbulent.
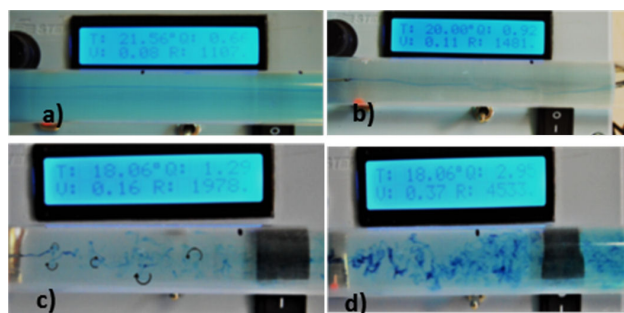

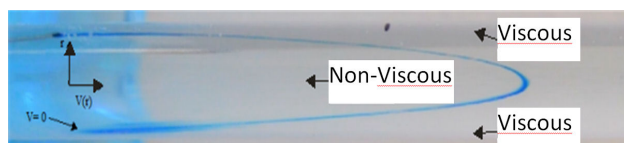FIGURE 14. a) laminar flow, Re = 1107, b) transient Re = 1481, c) turbulent Re = 1978, and d) turbulent Re = 4533.

FIGURE 15. Development of velocity profile in the pipe.

Several testing runs were carried out for different Re; in order to know about several fluid's parameters at any time, a display was implemented to measure them. Through this device, the user of the equipment is able to read fluid's veloc-ity, temperature and Re right from the screen, as depicted in Fig. 14. This is a core characteristic of the equipment since other equipments do not have such capability and the user can not know about fluid's characteristics.

On the other hand, velocity distribution in pipe's cross-sectional area can be visualized. The "no-sliding" effect can be observed so that ink particles next to pipe's wall adhere to it and stay at zero velocity, whereas velocity is maximum at the center of pipe, having a parabolic profile as shown in Fig. 15. It is also possible to see the development of the boundary layer in this figure; viscous and non-viscous zones are clearly distinguished, meaning that as flow increases, viscous layers unite and finally all the flow becomes viscous.

4. Conclusions

It was observed experimentally that working with fluids requires precision and close control of conditions in order to have coherent results, especially at high speeds ($1000 < Re < 10000$). At low speeds ($Re < 1000$), flow is laminar despite any disturbance may exist. This equipment was designed to work with Re numbers up to 23000, however, it was evident from testing runs that it is not necessary to use high Re numbers from a didactic standpoint, which is the main goal of this equipment; it permits observation of fluids behavior as well as reproduction of Osborne Reynolds' experiments carried out circa 1883 [20].

Flow velocity measurements has an error of $\pm10\%$ associated with flow meter. Microcontroller's working frequency is configured at 16 MHz to reduce error and to sense with enough speed since maximum frequency is 75 Hz. In the final characterization of the equipment, it was possible to measure Re numbers between 800 and 23000 as expected.

This design offers a novel way to visualize different flow types of incompressible fluids in piping since it allows the user to make readings directly from apparatus' screen. Temperature, velocity and Re are the parameters that can be taken. With this capability, users can verify theoretical calculations against data taken with the display; additionally they can easily realize as Re grows, fluid behavior changes from laminar to turbulent regime.

1. F.M. White, *Fluid Mechanics* (McGraw Hill, Seventh Edition, 2011).

2. Y.A. Cengel, J.M. Cimbala, *Fluid mechanics: Fundamentals and Applications* (McGraw Hill higher Education, Second Edition, 2010).

3. R.L. Mott, *Applied Fluid Mechanics* (Prentice Hall, Fifth Edition, 2000).

4. V.L. Streeter, E.B. Wylie, *Fluid Mechanics* (McGraw-Hill, Sixth Edition, 1975).

5. S.S. Rao, *The Finite Element Method in Engineering* (Butterworth Heinemann, Tercera edición, 1999).

6. L.J. Segerlind, *Applied Finite Element Analysis* (John Wiley and Sons, Segunda edición, 1984).

7. O.C. Zienkiewics, *The Finite Element Method* (Butterworth Heinemann, Quinta edición, 2000), **Vol. 1** The Basis.

8. Y. Nakasone, S. Yoshimoto, and T.A. Stolarski, *Engineering Analysis with Ansys software* (Elsevier, 2006).

9. *Ansys Fluent Tutorial Guide* (Ansys Inc., 2013).

10. G.O. Brown, *The History of the Darcy-Weisbach Equation for Pipe Flow Resistance, Environmental and Water Resources History* (Oklahoma State University, 2005).

11. C.F. Colebrook, *J. Inst. Civ. Eng.* **11** (1938) 4.

12. S.E. Haaland, *J. Fluids Eng.* **105** (1983) 1.

13. J. Nikuradse, *VDI-Forschungsheft 361. English Translation*, NACA Tech. Mem. (1933).

14. L.F. Moody, *ASME Trans.* **66** (1944).

15. Maxim Integrated, *Programmable Resolution 1-Wire Digital Thermometer*.

16. Olimex, Products-components. https://www.olimex.com/Products/Components/

17. ATMEL. *ATMEL 8-bit Microcontroller with 4/8/16/32 KBytes In-System Programmable Flash Datasheet*.

18. B.E. Hall, *Build a Dual Temperature Maxim DS18B20 Thermometer*.

19. G. Marull, *Using DS18B20 digital temperature sensor on AVR microcontrollers: Description and application* (September 2007).

20. O. Reynolds, *Phil. Trans. R. Soc.* **174** (1883).

21. Moody chart. Wikipedia. https://en.wikipedia.org/wiki/Moody_chart